NUTM1 is a recurrent fusion gene partner in B-cell precursor acute lymphoblastic leukemia associated with increased expression of genes on chromosome band 10p12.31-12.2

Femke M. Hormann,[1,2] Alex Q. Hoogkamer,[1,2] H. Berna Beverloo,[3] Aurélie Boeree,[1,2] Ilse Dingjan,[1,2] Moniek M. Wattel,[3] Ronald W. Stam,[1] Gabriele Escherich,[4] Rob Pieters,[1,5] Monique L. den Boer[1,2,5,6] and Judith M. Boer[1,2]

[1]Princess Máxima Center for Pediatric Oncology, Utrecht, the Netherlands; [2]Oncode Institute, Utrecht, the Netherlands; [3]Department of Clinical Genetics, Erasmus Medical Center, Rotterdam, the Netherlands; [4]COALL – German Cooperative Study Group for Childhood Acute Lymphoblastic Leukemia, Hamburg, Germany; [5]DCOG – Dutch Childhood Oncology Group, Utrecht, the Netherlands and [6]Department of Pediatric Oncology and Hematology, Erasmus Medical Center - Sophia Children's Hospital, Rotterdam, the Netherlands

Correspondence: JUDITH M. BOER. - j.m.boer-20@prinsesmaximacentrum.nl
doi:10.3324/haematol.2018.206961

SUPPLEMENTAL DATA
for

NUTM1 is a recurrent fusion gene partner in B cell precursor acute lymphoblastic leukemia associated with increased expression of genes on chromosome band 10p12.31-12.2

Femke M. Hormann[1,2], Alex Q. Hoogkamer[1,2], H. Berna Beverloo[3], Aurélie Boeree[1,2], Ilse Dingjan[1,2], Moniek M. Wattel[3], Ronald W. Stam[1], Gabriele Escherich[4], Rob Pieters[1,5], Monique L. den Boer[1,2,5,6], Judith M. Boer[1,2]

[1]Princess Máxima Center for pediatric oncology, Utrecht, The Netherlands
[2]Oncode Institute, The Netherlands
[3]Department of Clinical Genetics, Erasmus Medical Center, Rotterdam, The Netherlands
[4]COALL – German Cooperative Study Group for Childhood Acute Lymphoblastic Leukemia, Hamburg, Germany
[5]DCOG – Dutch Childhood Oncology Group, Utrecht, The Netherlands
[6]Department of Pediatric Oncology and Hematology, Erasmus Medical Center - Sophia Children's Hospital, Rotterdam, The Netherlands

CONTENT:

SUPPLEMENTAL METHODS

Patient cohort

Bone marrow and/or peripheral blood samples were obtained from children newly diagnosed with ALL. In accordance with the declaration of Helsinki, written informed consent to use excess diagnostic material for research purposes was obtained from parents or guardians, as approved by the Medical Ethics Committee of the Erasmus Medical Center, The Netherlands. This study comprised of children with newly diagnosed ALL in three consecutive Dutch Childhood Oncology Group trials (DCOG ALL-8, ALL-9, and ALL-10)[1], two German Cooperative ALL trials (COALL 06-97 and 07-03)[2] and the international infant ALL trial Interfant-99[3], as described.[4] The major known cytogenetic subtypes, *ETV6-RUNX1*, *TCF3-PBX1*, *KMT2A*/*MLL*-rearranged, *BCR-ABL1*, and high hyperdiploidy (51-67 chromosomes), were determined by reference laboratories using fluorescence in situ hybridization (FISH) and RT-PCR. Cases negative for these subtypes were classified as B-other-ALL. Within this B-other-ALL subgroup, *BCR-ABL1*-like cases were identified using the 110-probe set gene expression classifier as described.[4] RNA and DNA were isolated using Trizol reagents from mononuclear cells obtained by Lymphoprep density gradient centrifugation and enriched to >90% leukemic blasts.[5]

RNA sequencing

RNA from a population-based cohort of 71 pediatric ALL cases was used for paired-end 101-bp TruSeq Illumina strand-specific sequencing of ribosomal RNA-depleted total RNA using Illumina HiSeq 2000 with a median library size of 50 million read pairs according to the manufacturer's instructions. Fastq files were aligned to the GRCh37 reference using STAR 2.5.0b.[6] Read counts were determined with HTseq-count version 0.6.1p1. Fusion gene detection was performed by taking the overlap from STAR-Fusion 1.0.0 and FusionCatcher 0.99.7b results. Exon numbers relate to the *NUTM1* collapsed RefSeq reference (Supplemental Figure S2).

Affymetrix expression microarray

Expression microarrays (Affymetrix U133 Plus 2) were analyzed from a previously described population-based pediatric ALL cohort.[4,7] Differential gene expression between five *NUTM1*-positive cases and 112 *NUTM1*-negative B-other-ALL (excluding *BCR-ABL1*-like and hypodiploid (≤39 chromosomes)) cases was determined using Limma.[8] Probe sets with a false discovery rate (FDR) ≤0.01 were selected and analyzed for enrichment using DAVID.[9] An additional cohort of 70 infant ALL cases was used to study the expression of *NUTM1* and differentially expressed genes in infants.[10] Because the leukemic subtypes in the pediatric and the infant cohort, while in each separate cohort representative of the occurrence in the disease population, were not balanced, it was not possible to analyze these cohorts together.

Fluorescence in situ hybridization (FISH)

FISH was performed on cytospins of mononuclear cells using the *NUTM1* Breakapart probe set (MPH4800) by Cytocell (Cambridge, UK). Both probes located to 15q14; Red 34,263,646-34,415,095, Green 34,999,095-35,116,172 (Ensembl v.74.37/GRCh37). Nuclei were counterstained with DAPI.

Reverse transcriptase PCR

Primers were designed using primer3 and designed to amplify a region containing the fusion breakpoint with at least 100 bp of both fusion partners, for primer sequences see Supplemental Table S1. cDNA was

synthesized from RNA using M-MLV reverse transcriptase by Promega (Madison, WI) or the SensiFAST cDNA synthesis kit by Bioline (London, Great-Brittain). PCR was performed using Taq polymerase and PCR buffer II by Applied Biosystems (Bleiswijk, Netherlands). PCR products were purified using the QIAquick PCR Purification Kit by Qiagen (Venlo, Netherlands). Sanger sequencing was done by Macrogen (Amsterdam, Netherlands).

Immunofluorescence NUTM1 staining

Immunofluorescence staining was performed on archived cytospins. After thawing, the cytospins were fixed in 4% paraformaldehyde (PFA) in PBS for 15 min at room temperature. Cells were permeabilized with 0.5% Triton X-100 and blocked with confocal laser scanning microscopy buffer [PBS, 20 mM glycine and 3% BSA] for 30 min. For immunostaining, the cells were incubated with NUT C52B1 antibody (1:400, #3625, Cell Signaling Technology (Leiden, Netherlands)) in confocal laser scanning microscopy buffer overnight at 4°C. Subsequently, cells were washed with PBS and incubated with goat anti-rabbit IgG (H+L) Alexa fluor-647-conjugated antibody (1:400, A32733, ThermoFisher (Bleiswijk, Netherlands)) for 1 h at room temperature. Cells were embedded in ProLong Glass Antifade Mountant with NucBlue Stain (P36983, ThermoFisher). All samples were imaged with a Leica SP8 confocal laser scanning microscope with a 63×1.40 NA oil immersion objective (Leica HC PL APO 63×/1.40 CS2). All images were evaluated with Fiji (ImageJ v1.52i).

SUPPLEMENTAL TABLES

Supplemental table S1. Reverse transcription PCR primers used for the validation or identification of *NUTM1* fusions

Primer name	Sequence of primer	Reference sequence[1]
ACIN1 exon 1-2 FW	5'-GCTCAAAGGGGCTCTAATGC-3'	NM_001164814.1
AFF1 exon 13 FW	5'-GTCCTCGTCCTCCCAGAAG-3'	NM_005935.3
CUX1 exon 19 FW	5'-GCCATGGAGCAAGCTGAC-3'	NM_001202543.1
CUX1 exon 21 FW	5'-AAGGACAGCAAGCCACCA-3'	NM_001202543.1
CUX1 exon 23 FW	5'-CACCGAGTACAGCCAGGG-3'	NM_001202543.1
IKZF1 exon 1 FW	5'-GCGACGCACAAATCCACATA-3'	NM_006060.6
IKZF1 exon 5 FW	5'-CCCTTCAAATGCCACCTCTG-3'	NM_006060.6
SLC12A6 exon 2 FW	5'-CGGACCTCAGCTCTCGATC-3'	NM_001042494.1
ZNF618 exon 8 FW	5'-GGACGAGGTGAAGGAGGAG-3'	NM_133374.2
NUTM1 exon 3 RV	5'-GGTCAGAAGTTGGTGGGAGA-3'	NM_001284292.1
NUTM1 exon 3 RV.2	5'-CCGTCCCCTGTCACCAAC-3'	NM_001284292.1
NUTM1 exon 6 RV	5'-CAGGAGGTCTCTGGGCTTTA-3'	NM_001284292.1
NUTM1 exon 6 RV.2	5'-CTGCTGCCCTTCTTCCTCTT-3'	NM_001284292.1

[1] Reference sequence used for primer design and exon nomenclature

Supplemental Table S2. Results from the reverse transcription PCR and Sanger sequencing

Case	Fusion	Forward primer	Reverse primer	Sequence fusion partner[1]	Sequence *NUTM1*[1]
1	*SLC12A6* ex2 - *NUTM1* ex3	*SLC12A6* exon 2 FW	*NUTM1* exon 3 RV.2	5'-ACTGGATCCACCCAGTGACC GGACTTCTCACCCCCAGGATGTCA TCGAGG-3'	5'-CATCTGCATTGCCGGGACCGGAT ATGAGCATGAAACCTAGTGCCGCCC TG-3'
2	*CUX1* ex23 - *NUTM1* ex5	*CUX1* exon 23 FW	*NUTM1* exon 6 RV	5'-CAGCTCAACCTGAAAACCAG CACCGTCATCAACTGGTTCCACAA CTACAG-3'	5'-GTTCATGGAGTTTGAGGCTGAGG AGATGCAGATTCAGAACACACAGCT GA-3'
3	*CUX1* ex23 - *NUTM1* ex4	*CUX1* exon 23 FW	*NUTM1* exon 6 RV	5'-CAGCTCAACCTGAAAACCAG CACCGTCATCAACTGGTTCCACAA CTACAG-3'	5'-CCCAGTGCTTCGTTCCCTGGCCCG GCTGAAGCCCACTATGACCCTGGAG G-3'
4	*IKZF1* ex7 - *NUTM1* ex5	*IKZF1* exon 5 FW	*NUTM1* exon 6 RV.2	5'-ATCAGAGAGATNTNTCGTGC TGGACAGACTAGCAAGTAACGTC GCCAAAC-3'	5'-GTTCATGGAGTTTGAGGCTGAGG AGATGCAGATTCAGAACACACAGCT GA-3'
5	Negative for the following primer pairs: *SLC12A6* exon 2 FW, *NUTM1* exon 3 RV.2; *CUX1* exon 23 FW, *NUTM1* exon 6 RV; *CUX1* exon 19 FW, *NUTM1* exon 6 RV.2; *CUX1* exon 19 FW, *NUTM1* exon 3 RV.2; *CUX1* exon 21 FW, *NUTM1* exon 6 RV.2; *CUX1* exon 21 FW, *NUTM1* exon 3 RV.2; *IKZF1* exon 1 FW, *NUTM1* exon 3 RV.2; *IKZF1* exon 1 FW, *NUTM1* exon 6 RV.2; *IKZF1* exon 5 FW, *NUTM1* exon 3 RV.2; *IKZF1* exon 5 FW, *NUTM1* exon 6 RV.2; *ACIN1* exon 1-2 FW, *NUTM1* exon 6 RV.2; *AFF1* exon 13 FW, *NUTM1* exon 3 RV; *AFF1* exon 13 FW, *NUTM1* exon 6 RV.2; *ZNF618* exon 8 FW, *NUTM1* exon 6 RV				
6	NO MATERIAL AVAILABLE				
7	NO MATERIAL AVAILABLE				

[1] Results from Sanger sequencing using the forward primer, the 50 nucleotides adjacent to the fusion break point are given. Results were confirmed using the reverse primer.

Supplemental Table S3. 130 significantly differentially expressed probe sets (FDR ≤0.01) between pediatric *NUTM1*-positive vs *NUTM1*-negative cases, determined by Limma[8]

Probe set ID	Representative public ID	Alignments (GRCh37/hg19)	Gene symbol	Log2 FC[1]	P-value	Adjusted p-value[2]
231338_at	AL040313	chr15:34648899-34649933 (+) // 97.73 // q14	NUTM1	1.8	4.4E-40	2.4E-35
1559266_s_at	AI363206	chr10:21802406-21805716 (-) // 87.55 // p12.31	SKIDA1	2.3	1.3E-27	3.6E-23
231310_at	BF057073	chr3:32938602-32939315 (+) // 94.53 // p22.3	TRIM71	3.3	9.0E-25	1.6E-20
1558977_at	BM547591	chr10:22541000-22543518 (+) // 99.8 // p12.31	LOC100130992	1.3	8.8E-19	1.2E-14
239503_at	AI803010	chr10:21781588-21782103 (-) // 89.41 // p12.31	CASC10	1.2	1.0E-17	1.1E-13
218409_s_at	NM_022365	chr10:22045506-22209824 (-) // 98.74 // p12.31	DNAJC1	1.4	7.1E-16	6.5E-12
222621_at	BF591419	chr10:22045476-22292633 (-) // 92.63 // p12.31	DNAJC1	2.8	6.8E-14	5.3E-10
210033_s_at	AF079363	chr10:22634415-22706536 (+) // 99.96 // p12.2	SPAG6	1.8	5.4E-13	3.4E-09
231049_at	AI052253	chr11:33891635-33892061 (-) // 80.81 // p13	LMO2	1.3	5.6E-13	3.4E-09
222620_s_at	BF591419	chr10:22045476-22292633 (-) // 92.63 // p12.31	DNAJC1	2.8	9.9E-13	5.4E-09
210032_s_at	AI651156	chr10:22634415-22706539 (+) // 98.58 // p12.2	SPAG6	1.2	1.2E-12	5.4E-09
205938_at	NM_014906	chr17:56833231-57061026 (+) // 95.45 // q22	PPM1E	1.3	1.2E-12	5.4E-09
243431_at	BF000597	chr9:138981635-138982100 (-) // 94.98 // q34.3	---	0.9	4.6E-12	1.9E-08
1555923_a_at	BQ007522	chr10:21783420-21786193 (-) // 97.96 // p12.31	CASC10	0.7	4.9E-12	1.9E-08
220415_at	NM_015978	chr1:74701084-75010108 (+) // 98.97 // p31.1	FPGT-TNNI3K /// TNNI3K	1.8	7.4E-12	2.7E-08
230122_at	BE219716	chr10:21845268-21846111 (+) // 50.11 // p12.31	MLLT10	1.3	3.2E-11	1.0E-07
218847_at	NM_006548	chr3:185361774-185542812 (-) // 86.64 // q27.2	IGF2BP2	2.4	3.3E-11	1.0E-07
1564603_at	AK098568	chr15:34638191-34649929 (+) // 99.73 // q14	NUTM1	0.5	3.7E-11	1.1E-07
238257_at	N64035	chr10:22015634-22016029 (-) // 97.52 // p12.31	---	1.6	5.4E-11	1.6E-07
239611_at	AW149839	chr14:33990249-33990719 (+) // 95.89 // q13.1	---	0.8	8.1E-11	2.2E-07
215163_at	AK022211	chr3:185506525-185508293 (-) // 60.25 // q27.2	---	0.8	2.0E-10	5.2E-07
1559265_at	AI363206	chr10:21802406-21805716 (-) // 87.55 // p12.31	SKIDA1	0.8	3.5E-10	8.6E-07
202265_at	NM_005180	chr10:22610165-22620222 (+) // 94.88 // p12.2	BMI1 /// COMMD3-BMI1	2.2	5.0E-10	1.2E-06
1556826_s_at	AW005545	chr1:11782186-11785384 (+) // 43.51 // p36.22	DRAXIN	0.7	1.1E-09	2.5E-06
235521_at	AW137982	chr7:27146626-27147537 (-) // 92.04 // p15.2	HOXA3	1.4	1.3E-09	2.8E-06
242216_at	AI791832	chr10:22201914-22202368 (-) // 99.34 // p12.31	---	2.7	2.1E-09	4.3E-06
213056_at	AU145019	chr3:69219145-69435224 (-) // 96.4 // p14.1	FRMD4B	-2.6	2.1E-09	4.3E-06

1566482_at	AL833114	chr12:65675436-65680508 (+) // 73.09 // q14.3	RP11-305O6.3	0.8	2.5E-09	4.9E-06
240788_at	AI076834	chr6:84050612-84051037 (-) // 35.93 // q14.2	---	0.7	3.9E-09	7.4E-06
218048_at	NM_012071	chr10:22605337-22609230 (+) // 96.46 // p12.2	COMMD3	1.8	4.4E-09	7.9E-06
235753_at	AI492051	chr7:27193339-27194232 (-) // 93.56 // p15.2	HOXA7	0.9	4.7E-09	8.3E-06
213150_at	BF792917	chr7:27210223-27214191 (-) // 95.91 // p15.2	HOXA10	2.1	5.5E-09	9.4E-06
213823_at	H94842	chr7:27220775-27222472 (-) // 94.68 // p15.2	HOXA11	1.1	6.5E-09	1.1E-05
1554127_s_at	BC040053	chr12:65672521-65857168 (+) // 94.28 // q14.3	MSRB3	0.7	8.9E-09	1.4E-05
213147_at	AI375919	chr7:27210223-27214191 (-) // 95.91 // p15.2	HOXA10	0.9	1.7E-08	2.6E-05
216503_s_at	AF060927	chr10:21823677-21827841 (+) // 64.76 // p12.31	MLLT10	1.1	1.8E-08	2.7E-05
223075_s_at	AL136566	chr9:133971928-133998530 (+) // 90.27 // q34.12	AIF1L	1.3	2.3E-08	3.3E-05
1560250_s_at	BC035844	chr18:29522537-29524117 (+) // 83.08 // q12.1	LOC284242	1.6	2.3E-08	3.4E-05
214651_s_at	U41813	chr7:27202219-27209269 (-) // 94.7 // p15.2	HOXA10-HOXA9 /// HOXA9 /// MIR196B	2.9	3.3E-08	4.6E-05
236302_at	R40892	chr17:57062093-57062532 (+) // 96.06 // q22	PPM1E	1.6	4.4E-08	6.1E-05
213059_at	AF055009	chr11:46337211-46342970 (+) // 83.57 // p11.2	CREB3L1	0.8	4.8E-08	6.4E-05
1554340_a_at	BC021286	chr1:11769390-11780631 (+) // 64.91 // p36.22	DRAXIN	1.3	5.0E-08	6.5E-05
219167_at	NM_016563	chr15:65345676-65360289 (-) // 94.32 // q22.31	RASL12	0.5	6.1E-08	7.7E-05
213844_at	NM_019102	chr7:27180687-27183283 (-) // 97.8 // p15.2	HOXA5	1.4	9.2E-08	1.1E-04
221104_s_at	NM_018376	chr9:107526416-107536129 (+) // 99.68 // q31.1	NIPSNAP3B	1.9	9.7E-08	1.2E-04
1553808_a_at	NM_145285	chr10:101292693-101296278 (+) // 92.06 // q24.2	NKX2-3	0.9	1.3E-07	1.5E-04
210472_at	BC005311	chr16:56700649-56701977 (-) // 96.53 // q13	MT1G	0.7	1.4E-07	1.6E-04
217546_at	R06655	chr16:56666144-56667893 (+) // 84.27 // q12.2	MT1M	1.0	1.6E-07	1.8E-04
204918_s_at	NM_004529	chr9:20344967-20622450 (-) // 93.78 // p21.3	MLLT3	0.9	1.6E-07	1.8E-04
202890_at	AW242297	chr6:136663551-136872247 (-) // 97.27 // q23.3	MAP7	1.2	2.1E-07	2.3E-04
206678_at	NM_000806	chr5:161274404-161324584 (+) // 99.78 // q34	GABRA1	0.5	2.4E-07	2.6E-04
231517_at	AW243917	chr1:53359785-53360247 (+) // 100.0 // p32.3	ZYG11A	0.5	2.6E-07	2.7E-04
209905_at	AI246769	chr7:27202056-27205149 (-) // 98.61 // p15.2	HOXA10-HOXA9 /// HOXA9 /// MIR196B	1.9	2.9E-07	2.9E-04
201690_s_at	AA524023	chr8:80947571-81083777 (-) // 97.78 // q21.13	TPD52	-1.8	2.9E-07	2.9E-04
236207_at	BE083088	chr2:182756922-182766664 (+) // 74.29 // q31.3	SSFA2	1.0	3.0E-07	3.0E-04
204249_s_at	NM_005574	chr11:33880124-33913836 (-) // 97.57 // p13	LMO2	2.3	3.3E-07	3.2E-04
225790_at	AL048386	chr12:65858090-65860687 (+) // 90.13 // q14.3	MSRB3	0.7	4.1E-07	3.9E-04

213836_s_at	AW052084	chr17:66417421-66417880 (-) // 95.03 // q24.2	WIPI1	1.5	5.5E-07	5.2E-04
1561956_at	AF085947	chr14:33433406-33434030 (+) // 41.48 // q13.1	---	0.7	5.9E-07	5.4E-04
217422_s_at	X52785	chr19:35822918-35837669 (+) // 99.53 // q13.12	CD22	-2.0	6.1E-07	5.5E-04
221035_s_at	NM_031272	chr17:56634039-56679869 (-) // 97.01 // q22	TEX14	0.9	6.6E-07	5.9E-04
204581_at	NM_001771	chr19:35822918-35838262 (+) // 97.02 // q13.12	CD22	-1.8	7.2E-07	6.3E-04
211748_x_at	BC005939	chr9:139872021-139876193 (+) // 95.74 // q34.3	PTGDS	0.7	8.4E-07	7.3E-04
201689_s_at	BE974098	chr8:80947571-81083777 (-) // 97.78 // q21.13	TPD52	-1.8	8.9E-07	7.6E-04
230412_at	BF196935	chr14:34271098-34271599 (+) // 97.01 // q13.1	NPAS3	0.8	9.0E-07	7.6E-04
223764_x_at	BC005202	chr9:107526488-107536134 (+) // 97.86 // q31.1	NIPSNAP3B	2.2	1.0E-06	8.4E-04
205773_at	NM_014912	chr10:93808398-94003003 (-) // 96.01 // q23.32	CPEB3	1.5	1.1E-06	8.7E-04
238021_s_at	AA954994	chr16:54952778-54962690 (-) // 97.39 // q12.2	CRNDE	-2.1	1.1E-06	8.8E-04
1555250_a_at	BC036444	chr10:93809389-94050844 (-) // 95.91 // q23.32	CPEB3	1.0	1.7E-06	1.3E-03
229281_at	N51682	chr14:34272419-34273382 (+) // 97.09 // q13.1	NPAS3	0.8	1.8E-06	1.4E-03
227999_at	AI290476	chr10:134230785-134231367 (+) // 93.45 // q26.3	PWWP2B	1.5	2.0E-06	1.5E-03
244118_at	AV722228	chr5:161325678-161326681 (+) // 99.3 // q34	GABRA1	0.5	2.3E-06	1.7E-03
1554862_at	BC022302	chr6:25127071-25138557 (-) // 83.79 // p22.3	CMAHP	0.6	2.3E-06	1.7E-03
203827_at	NM_017983	chr17:66417422-66453626 (-) // 99.95 // q24.2	WIPI1	1.0	2.4E-06	1.8E-03
240633_at	AI743416	chr4:3495780-3496209 (+) // 94.66 // p16.3	DOK7 /// LOC102724043	1.4	2.6E-06	1.9E-03
213248_at	AL577024	chr6:52531318-52533951 (+) // 85.34 // p12.2	LOC730101	0.9	2.7E-06	1.9E-03
1558368_s_at	AK075558	chr1:11751780-11786209 (+) // 76.21 // p36.22	DRAXIN	0.6	2.8E-06	2.0E-03
228293_at	AJ245600	chr11:33037408-33055126 (+) // 95.85 // p13	DEPDC7	1.0	3.0E-06	2.1E-03
238218_at	AW206656	chr6:74078281-74079083 (-) // 96.23 // q13	OOEP	0.4	3.2E-06	2.2E-03
218468_s_at	AF154054	chr15:33010280-33026058 (+) // 97.58 // q13.3	GREM1	2.6	3.3E-06	2.3E-03
239950_at	AW137133	chr7:27225035-27226472 (+) // 98.64 // p15.2	HOXA11-AS	0.6	3.4E-06	2.3E-03
212993_at	AA114166	chr9:138898384-138902358 (-) // 92.34 // q34.3	NACC2	0.5	3.4E-06	2.3E-03
235597_s_at	AU157274	---	RGPD1 /// RGPD2	0.8	3.9E-06	2.5E-03
214639_s_at	S79910	chr7:27132933-27135531 (-) // 97.4 // p15.2	HOXA1	0.7	3.9E-06	2.5E-03
201688_s_at	BG389015	chr8:80947571-81083777 (-) // 97.78 // q21.13	TPD52	-1.6	3.9E-06	2.5E-03
210524_x_at	AF078844	chr17:61895118-61895671 (-) // 51.26 // q23.3	---	1.4	4.3E-06	2.7E-03
201691_s_at	NM_005079	chr8:80947748-81083769 (-) // 99.26 // q21.13	TPD52	-1.2	4.3E-06	2.7E-03
219793_at	NM_022133	chr8:82712957-82752448 (-) // 99.63 // q21.13	SNX16	1.2	4.5E-06	2.8E-03
204917_s_at	AV756536	chr9:20344967-20622451 (-) // 93.84 // p21.3	MLLT3	1.0	4.5E-06	2.8E-03

222692_s_at	BF444916	chr3:172052787-172116573 (+) // 92.02 // q26.31	FNDC3B /// LOC101928615	0.4	4.5E-06	2.8E-03
1561708_at	BC012928	chr6:74123244-74161982 (-) // 97.15 // q13	MB21D1	0.8	5.0E-06	3.0E-03
212526_at	AK002207	chr13:36877001-36920420 (-) // 95.79 // q13.3	SPG20	1.9	6.1E-06	3.6E-03
1561606_at	BC042014	chr17:57043311-57044080 (+) // 76.67 // q22	RP11-579O24.3	0.4	6.2E-06	3.7E-03
213997_at	AB011146	chr15:29412456-29488755 (-) // 99.03 // q13.1	FAM189A1	0.6	6.5E-06	3.7E-03
218469_at	NM_013372	chr15:33010301-33026866 (+) // 99.65 // q13.3	GREM1	2.8	6.4E-06	3.7E-03
236418_at	AW772075	chr1:1119381-1132928 (+) // 98.73 // p36.33	TTLL10	0.4	6.9E-06	3.9E-03
243110_x_at	AI868441	chr16:2069627-2070750 (+) // 89.05 // p13.3	NPW	0.8	7.4E-06	4.1E-03
229744_at	AL556611	chr2:182758544-182759422 (+) // 97.56 // q31.3	SSFA2	1.7	7.6E-06	4.2E-03
224553_s_at	AF117297	chr1:1139223-1141951 (-) // 100.0 // p36.33	TNFRSF18	0.8	7.9E-06	4.3E-03
214033_at	AI084637	chr16:18582562-18584841 (+) // 84.32 // p12.3 /// chr16:16315046-16317326 (-) // 84.46 // p13.11 /// chr16:14916283-14918561 (-) // 84.18 // p13.11	ABCC6 /// ABCC6P1 /// ABCC6P2 /// LOC101930322	0.4	7.9E-06	4.3E-03
244414_at	AI148006	chr11:96019807-96020266 (-) // 89.63 // q21	---	-1.8	8.8E-06	4.7E-03
90265_at	AW050627	chr7:937544-938021 (-) // 90.25 // p22.3	ADAP1	0.7	9.5E-06	5.1E-03
1554905_x_at	BC033851	chr11:65154107-65154728 (+) // 86.03 // q13.1	FRMD8	1.4	9.8E-06	5.1E-03
226546_at	BG477064	chr12:58325231-58329950 (-) // 53.46 // q14.1	LOC100506844	1.8	9.7E-06	5.1E-03
229015_at	BF510739	chr9:107539001-107540045 (+) // 84.95 // q31.1	LOC286367	1.5	9.8E-06	5.1E-03
241987_x_at	BF029081	chr8:101585412-101596388 (-) // 96.52 // q22.2	SNX31	0.6	1.0E-05	5.2E-03
237600_at	AI023295	chr10:21893566-21894015 (+) // 30.95 // p12.31	---	1.0	1.1E-05	5.7E-03
216506_x_at	AF060938	chr10:21823677-21884313 (+) // 71.22 // p12.31	MLLT10	0.5	1.2E-05	5.8E-03
204745_x_at	NM_005950	chr16:56700652-56701977 (-) // 99.24 // q13	MT1G	2.0	1.2E-05	5.9E-03
227877_at	AI991103	chr5:43039334-43040127 (-) // 94.03 // p12	ANXA2R	1.3	1.2E-05	6.0E-03
214228_x_at	AJ277151	chr1:1146719-1149533 (-) // 98.26 // p36.33	TNFRSF4	0.5	1.3E-05	6.2E-03
216336_x_at	AL031602	chr1:33416742-33417152 (-) // 98.8 // p35.1	MT1E	1.6	1.3E-05	6.2E-03
225782_at	AW027333	chr12:65858090-65860687 (+) // 90.13 // q14.3	MSRB3	1.3	1.4E-05	6.6E-03
1568900_a_at	BC031218	chr19:37407242-37441256 (+) // 96.53 // q13.12	ZNF568	-0.8	1.4E-05	6.6E-03
204059_s_at	NM_002395	chr6:83921256-84140780 (-) // 95.75 // q14.2	ME1	0.5	1.4E-05	6.6E-03
38521_at	X59350	chr19:35822918-35838262 (+) // 93.58 // q13.12	CD22	-1.3	1.5E-05	6.8E-03
219686_at	NM_018401	chr4:5053526-5502725 (+) // 85.95 // p16.2	STK32B	-1.7	1.5E-05	6.9E-03
220316_at	NM_022123	chr14:33408458-34270951 (+) // 96.94 // q13.1	NPAS3	0.5	1.6E-05	7.2E-03
222315_at	AW972855	---	LOC100996756	1.4	1.6E-05	7.3E-03

236600_at	AI651603	chr13:36875777-36876234 (-) // 11.73 // q13.3	SPG20	0.6	1.6E-05	7.4E-03
241244_at	AI809328	chr2:170681667-170683756 (+) // 89.55 // q31.1	---	0.3	1.7E-05	7.7E-03
1557566_at	BC040313	chr1:55681079-55683126 (+) // 85.57 // p32.3	LOC100507634	0.7	1.7E-05	7.8E-03
224746_at	AB040955	chr1:33231267-33240806 (+) // 98.65 // p35.1	KIAA1522	0.5	1.8E-05	8.0E-03
204306_s_at	NM_004357	chr11:834526-838830 (+) // 86.54 // p15.5	CD151	0.4	2.0E-05	8.5E-03
226123_at	AI870918	chr8:61591400-61714142 (+) // 99.79 // q12.1	CHD7	-1.2	1.9E-05	8.5E-03
212859_x_at	BF217861	chr16:56659395-56661024 (+) // 89.43 // q12.2	MT1E	1.8	2.0E-05	8.6E-03
211822_s_at	AF229061	chr17:5418073-5487277 (-) // 98.07 // p13.2	NLRP1	-0.9	2.1E-05	8.9E-03
209502_s_at	BC002495	chr17:79008971-79090024 (+) // 97.23 // q25.3	BAIAP2	0.4	2.2E-05	9.3E-03
207850_at	NM_002090	chr4:74902313-74904405 (-) // 92.86 // q13.3	CXCL3	1.6	2.3E-05	9.9E-03
207729_at	NM_016279	chr5:26880708-27038674 (-) // 97.91 // p14.1	CDH9	0.4	2.4E-05	1.0E-02

[1] Log2 FC pediatric *NUTM1*-positive cases (n=5) versus pediatric *NUTM1*-negative B-other-ALL cases (n=112)
[2] Genes are ordered on adjusted P-value (Benjamini-Hochberg), ascending

SUPPLEMENTAL FIGURE LEGENDS

Supplemental Figure S1. Integrative genomic viewer image of reads mapped to *NUTM1*
Total RNA sequencing reads were aligned with STAR and visualized with Integrative Genomic Viewer (version 2.4.10, hg19). *NUTM1* expression of case 1 (*SLC12A6-NUTM1* fusion case; index case) and a control case without a *NUTM1* fusion is shown.

Supplemental Figure S2. FISH results for *NUTM1* break-apart probes
(A) *NUTM1* FISH probe locations on chromosome band 15q14. UCSC genome browser view of chromosome location (first track), locations of the break-apart probe sets (second track), locations of the fusion genes (third track), chromosome band (fourth track), and UCSC genes (fifth track) aligned to GRCh37/hg19. **(B)** Representative microscopic images for each of the five cases for which FISH was performed. **(C)** Summarized FISH results for 76-100 counted nuclei. F, fusion signal, both signals located on top of each other; GR, fusion signal, both signals located directly next to each other; G, green signal located alone; R, red signal located alone.

Supplemental Figure S3. *HOXA* cluster expression in *NUTM1* fusion cases
(A) Heatmap of the expression of *NUTM1* and *HOXA* genes upregulated in *NUTM1*-positive versus *NUTM1*-negative cases (FDR ≤0.01) in the pediatric population-based cohort. Expression of these genes is shown for the infant cohort as well. Log2 values were centered around 0 using the median of B-other-ALL cases and *NUTM1* fusion cases and scaled by 2x root-mean-square for the population-based cohort and the infant ALL cohort individually. Blue indicates reduced expression, red indicates increased expression compared with the median of all included cases per cohort. Within the *HOXA* cluster, genes are ordered by genomic location. **(B)** Visualization of all probe sets within the 7p14-p15 chromosome band. UCSC genome browser view of chromosome location (first track), probe sets (second track), chromosome band (third track), and UCSC genes (fourth track) aligned to GRCh37/hg19. In the second track, all probe sets that map to the location in this view are visualized. Each probe set is visualized with a thick band from start to end and arrows indicating the strand. Black band means no different expression between *NUTM1*-positive and *NUTM1*-negative cases, red means increased expression in *NUTM1*-positive cases versus *NUTM1*-negative cases (FDR ≤0.01).

Supplemental Figure S4. Expression of differentially expressed genes related to *NUTM1* expression
Dot plots showing the *NUTM1* expression (Affymetrix probe set 231338_at) on the x-axis and the expression of one of the selected genes on the y-axis for B-other-ALL cases (grey) and *NUTM1*-positive cases (colored, same colors and symbols as in Figure 1C). Left panels show the pediatric cohort and the right panels show the infant ALL cohort. Genes are selected based on the gene expression comparison between the five *NUTM1*-positive pediatric BCP-ALL cases to the remaining 112 *NUTM1*-negative pediatric B-other-ALL cases and shown for the infant cohort in comparison.

SUPPLEMENTAL FIGURES

Supplemental Figure S1. Integrative genomic viewer image of reads mapped to *NUTM1*

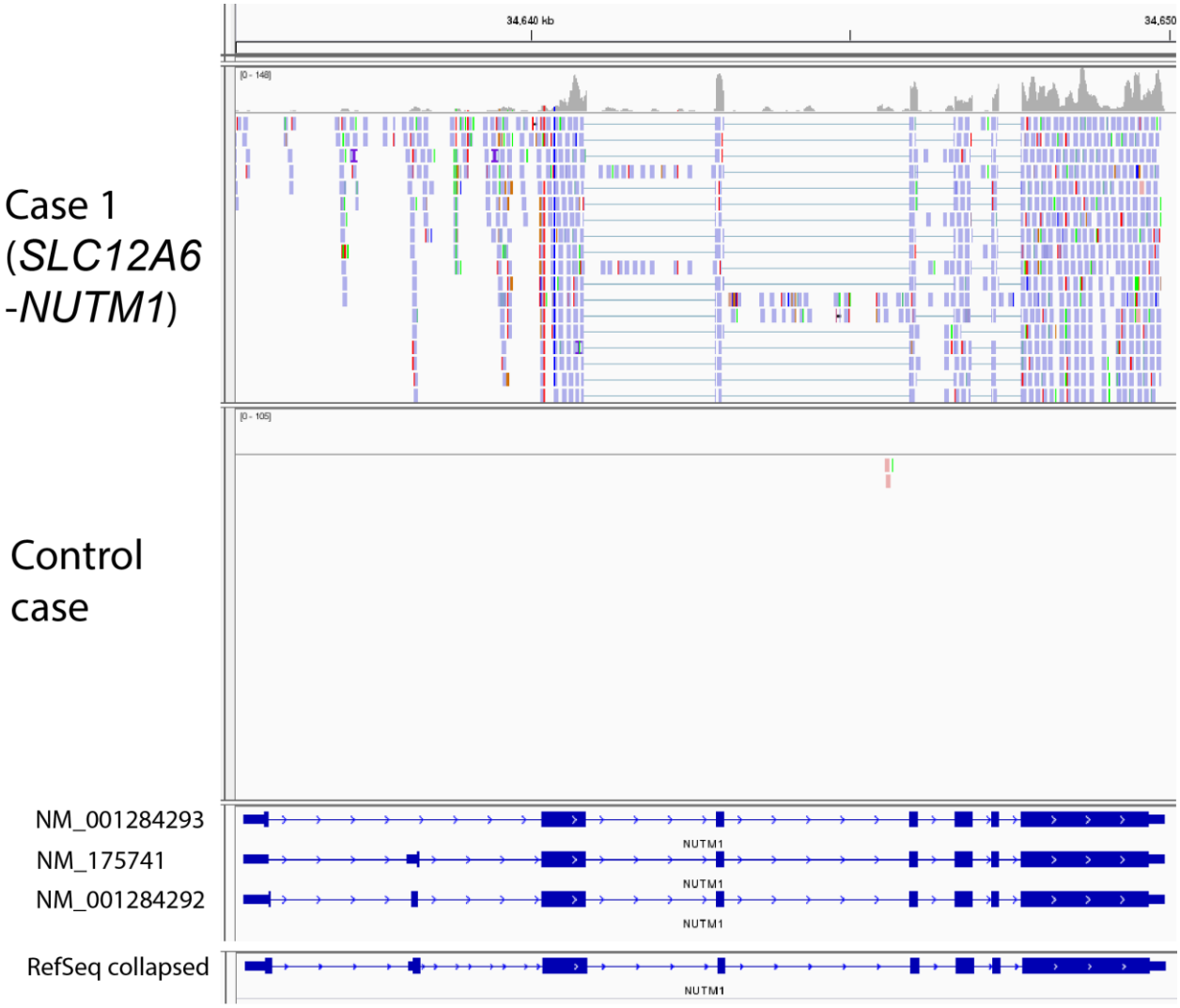

Supplemental Figure S2. FISH results for *NUTM1* break-apart probes

A

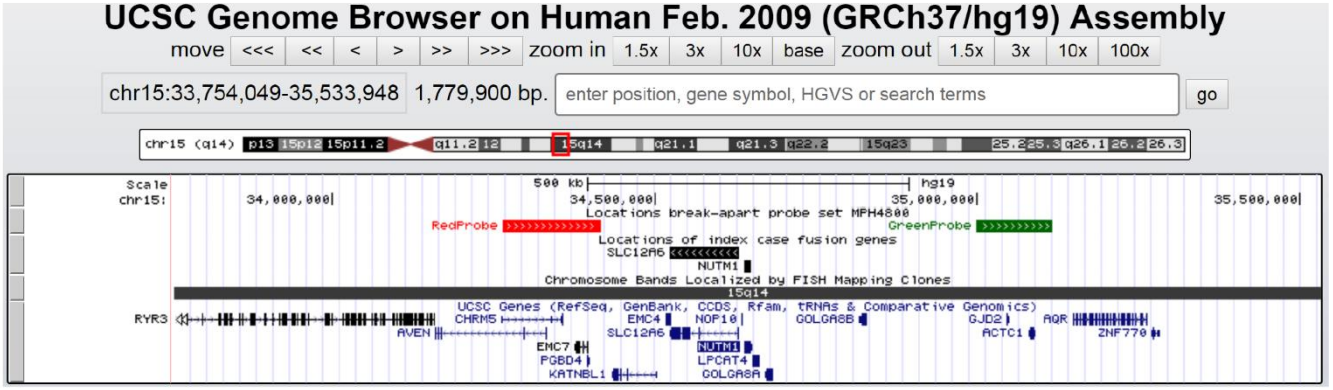

B

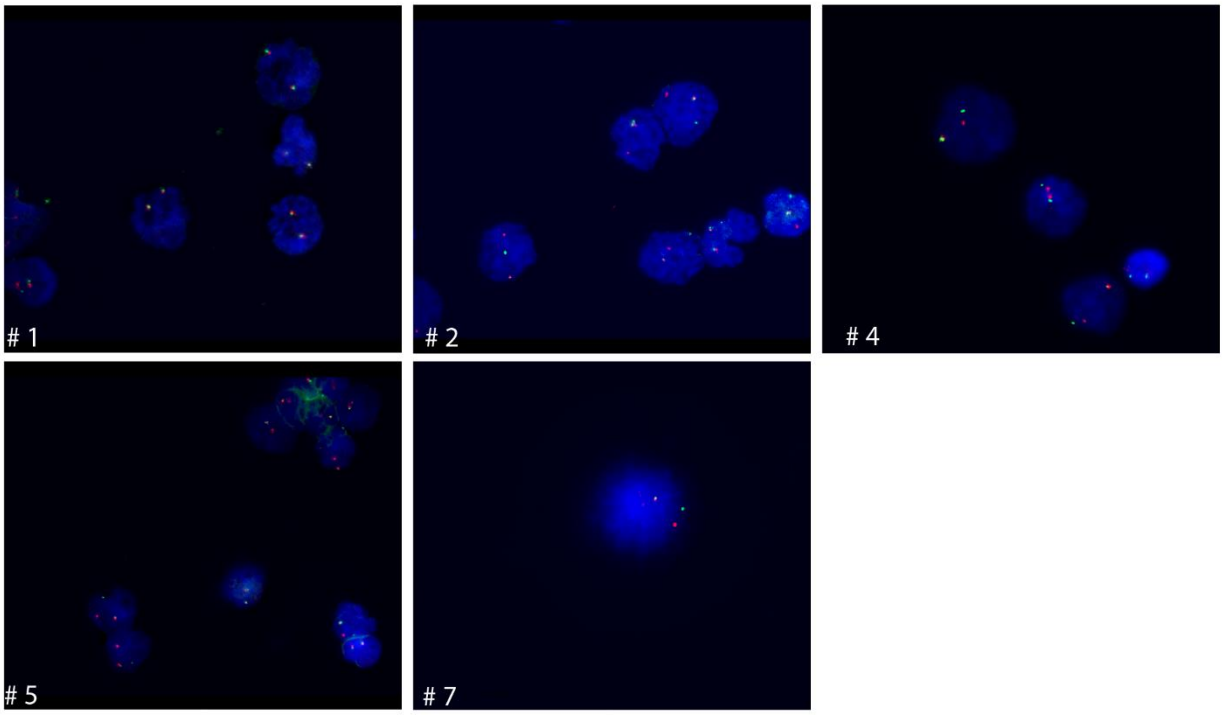

C

Case	Nuclei counted	F F	F GR	GR GR	F G R	GR G R
1	100	90	8	2		
2	100			4	92	
4	100			43		53
5	100			22		71
7	76			44		26

Supplemental Figure S3. *HOXA* cluster expression in *NUTM1* fusion cases

A

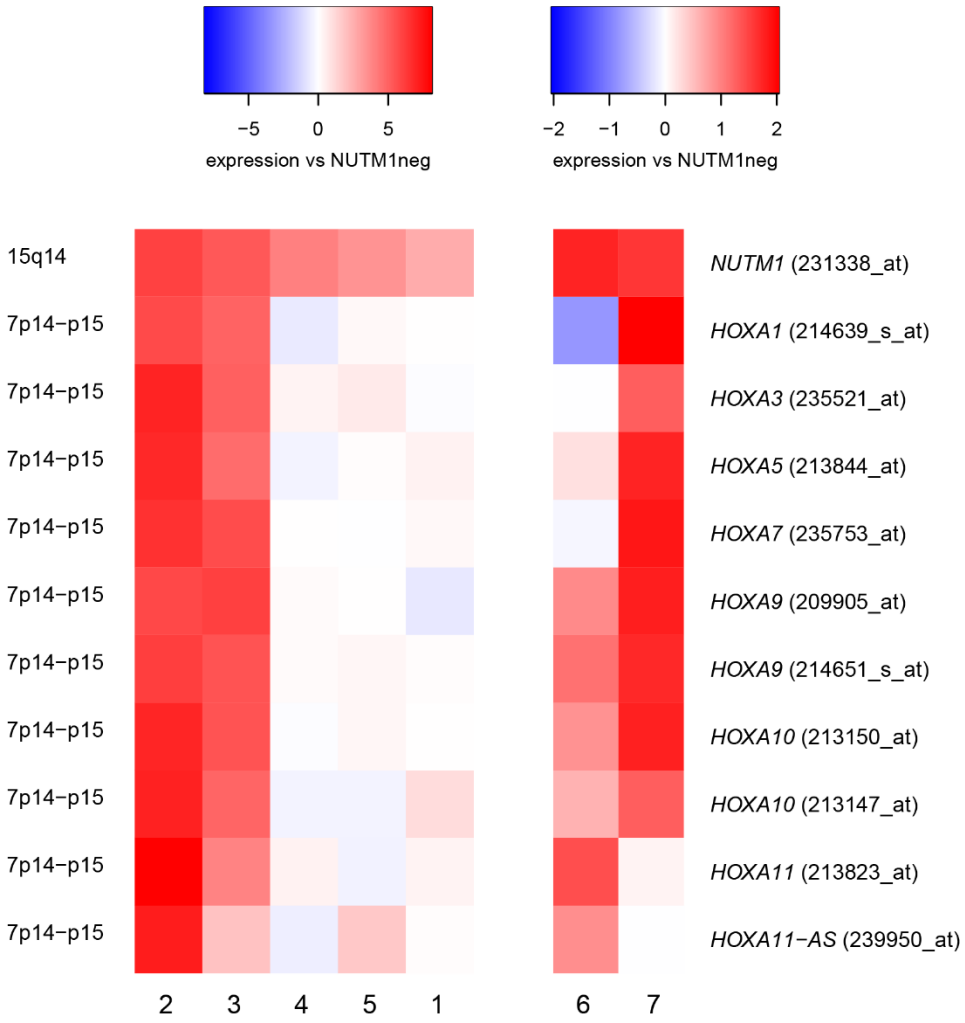

B

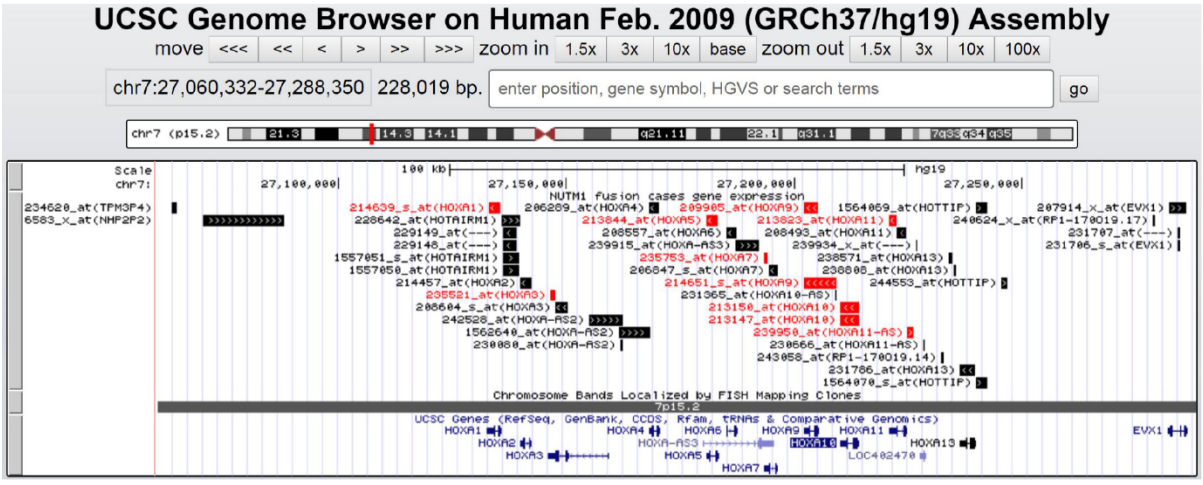

Supplemental Figure S4. Expression of differentially expressed genes related to *NUTM1* expression

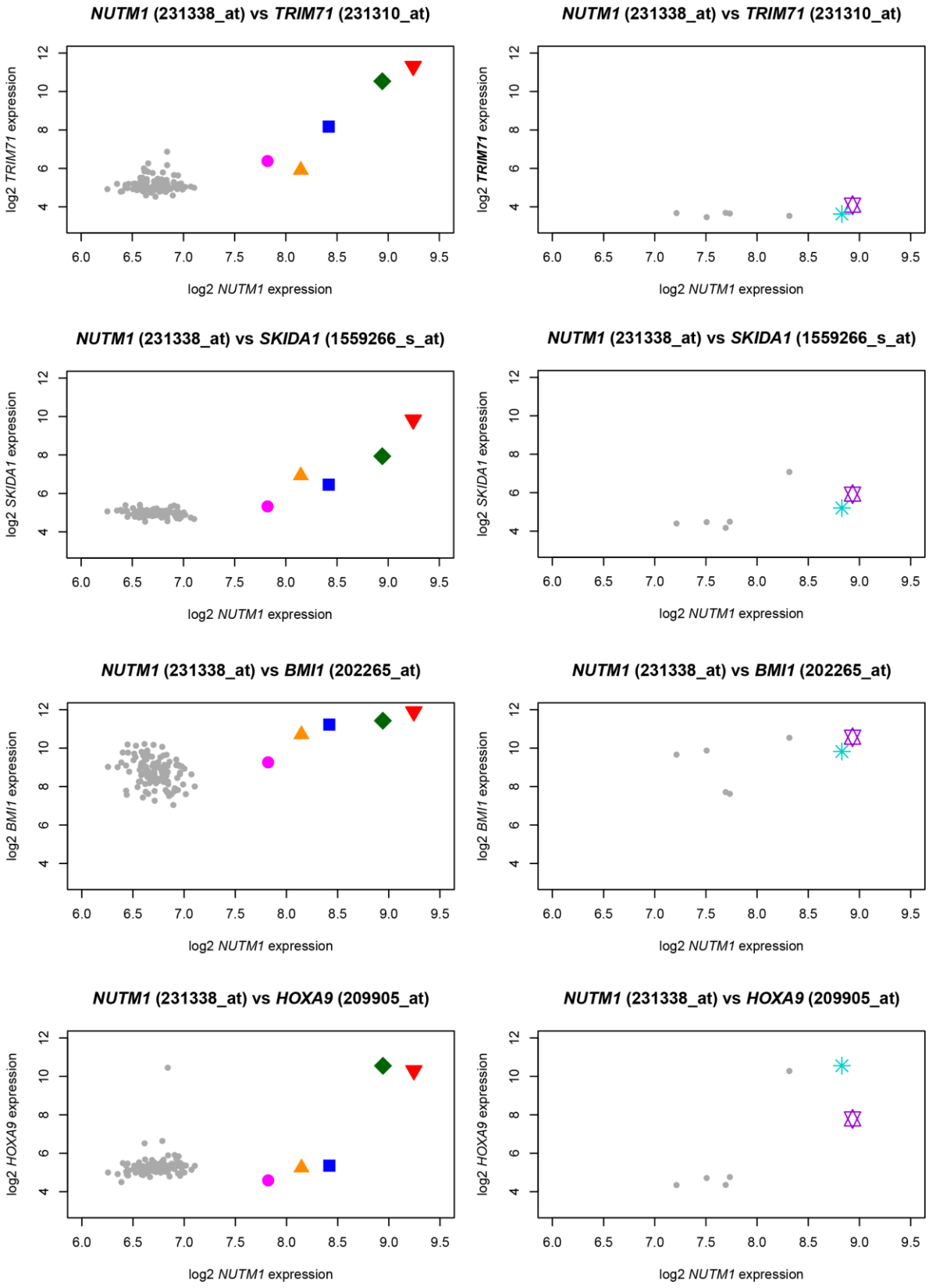

SUPPLEMENTAL REFERENCES

1. Kamps WA, van der Pal-de Bruin KM, Veerman AJP, Fiocco M, Bierings M, Pieters R. Long-term results of Dutch Childhood Oncology Group studies for children with acute lymphoblastic leukemia from 1984 to 2004. Leukemia 2010;24(2):309–19.
2. Escherich G, Horstmann MA, Zimmermann M, Janka-Schaub GE, COALL study group. Cooperative study group for childhood acute lymphoblastic leukaemia (COALL): long-term results of trials 82,85,89,92 and 97. Leukemia 2010;24(2):298–308.
3. Pieters R, Schrappe M, De Lorenzo P, et al. A treatment protocol for infants younger than 1 year with acute lymphoblastic leukaemia (Interfant-99): an observational study and a multicentre randomised trial. Lancet (London, England) 2007;370(9583):240–250.
4. van der Veer A, Waanders E, Pieters R, et al. Independent prognostic value of BCR-ABL1-like signature and IKZF1 deletion, but not high CRLF2 expression, in children with B-cell precursor ALL. Blood 2013;122(15):2622–9.
5. Den Boer ML, Harms DO, Pieters R, et al. Patient stratification based on prednisolone-vincristine-asparaginase resistance profiles in children with acute lymphoblastic leukemia. J Clin Oncol 2003;21(17):3262–8.
6. Dobin A, Davis CA, Schlesinger F, et al. STAR: ultrafast universal RNA-seq aligner. Bioinformatics 2013;29(1):15–21.
7. Steeghs EMP, Bakker M, Hoogkamer AQ, et al. High STAP1 expression in DUX4-rearranged cases is not suitable as therapeutic target in pediatric B-cell precursor acute lymphoblastic leukemia. Sci Rep 2018;8(1):693.
8. Smyth GK. limma: Linear Models for Microarray Data. In: Bioinformatics and Computational Biology Solutions Using R and Bioconductor. New York: Springer-Verlag; p397–420.
9. Huang DW, Sherman BT, Lempicki RA. Systematic and integrative analysis of large gene lists using DAVID bioinformatics resources. Nat Protoc 2009;4(1):44–57.
10. Stam RW, Schneider P, Hagelstein JAP, et al. Gene expression profiling-based dissection of MLL translocated and MLL germline acute lymphoblastic leukemia in infants. Blood 2010;115(14):2835–44.